

Performance Computations and Design Criterion of Airfoils in Unsteady Viscous Flows

Rosario M. A. Marretta¹, Giovanni Lombardi² and Roberto Antinoro¹

Abstract: An approach based on Lighthill's transpiration velocity is explored and proposed for a new design criterion for airfoils in unsteady and viscous flows. This criterion confines its methodologies to the close proximity of the laminar and turbulent boundary layer and it shows good efficiency in predicting and calculating the wake evolution regions in a wide range of operating unsteady parameters. Also, the criterion is capable of predicting low Mach number, attached flow-fields as accurately as the full Navier-Stokes solutions when the massive flow separation is avoided. The agreement of the present results with those empirically and theoretically determined is very accurate for attached flows and well within the general range of the boundary layer correlations and the angles of attack of the airfoils. Finally, the proposed computational recursive scheme is unusually not sensitive to the order of discretization and the distribution of the nodes and, under the hypotheses of work, it makes possible a complete and quite well description of the vortical regions of the wake past the airfoil under several unsteady starting conditions which may be iterated to give accurate results reliability.

keyword: Unsteady, Viscous, Flow, Airfoils.

1 Introduction

Present day computational fluid dynamic methods are suitable of investigating and predicting the details of separated flows and the necessity for detachment criteria and information is diminishing correspondingly. It is important to emphasize that CFD prediction of separated flows still requires highly sophisticated codes and powerful (sometimes dedicated) computational machines.

Flow separation is the single most important factor that

limits the efficiency and operating range of fluid dynamic devices and their design. For many decades, this problem occupied a large share of fluid mechanics research. Although much progress has been made, the prediction of the occurrence of separation in all circumstances still has not been reached and the investigation of the physics and the mechanisms of the laminar and turbulent separation processes goes on [Sajben and Liao (1995)]. A comprehensive review of the state of the art of this field, for the computational applications of the Boundary Integral Equations (*BIE*), was given by Morino [Morino (1993)]. While integral theories give fast, and, in many cases, quite well adequate solutions with the use of minimal human and computational resources, the method of their choice remains a crucial step in many industrial situations dominated by cost-time constraints. The original motivation for this paper was aimed at giving a physically plausible and fast-computationally design criterion for evaluating the airfoils performance in unsteady and viscous flows with reasonable fast computational time of convergence. The reasonable success of the proposed methodology grew out of the intuitive expectation that boundary layer exposed to adverse pressure gradients will detach if the momentum carried out by the boundary layer becomes less than some fraction of the free-stream momentum. The ideas offered in the present work are related with design methodologies and criteria regarding (and treating) this expectation as a guideline, cast it into a quantitative form with convenient parameters and compare the calculations to establish theoretical and experimental results. Before focusing on the aim of the present work, let us review briefly the methodologies and criteria used in incompressible viscous flows. Generally, the objective is a suitable (and appropriate) combination of the Helmholtz and the Poincaré decomposition. These are particular cases of the general potential-vorticity decomposition of the velocity field into a superposition of a potential velocity and a vortical velocity which is a particular solution of the equation involving the vorticity dis-

¹ Department of Mechanics and Aeronautics, Viale delle Scienze, 90128 Palermo, Italy.

² Department of Aerospace Engineering, Via Caruso, 56122 Pisa, Italy.

tribution. The previous formulation is similar to those for compressible flows. In order to extend the potential-flow formulation, it is necessary an extension to viscous flows of the Bernoulli's theorem for compressible flows, rewriting the Navier-Stokes (N-S in the following) equations in terms of the viscous stress tensor. In the N-S/potential flow interactive scheme [Tuncer, Ekaterinaris and Platzer (1995)], the computational domain is splitted into two zones, a near field and a far field zone so as to reduce to one-fifth of a chord length around the airfoil surface the computational domain (in comparison to the full N-S solvers in which the processed domain is required to extend approximately 15 chord lengths from the airfoil surface). If this method is applied to unsteady flows, it is essential to model the vortex shedding and the viscous wake, whereas, for steady flow-fields, no vortex shedding investigation is required. This paper focuses on the case of two-dimensional flow and approaches the unsteady and viscous problem with the methods of "flow reduction" of Lighthill [Lighthill (1958)]. Taking into account the aerodynamic performance parameters of the airfoils, the displacement-thickness theory, mentioned above, seems a real advantage for design purpose when the considerations are limited only to the response of airfoils in unsteady and viscous flow. Here, the investigation of the evolution of the boundary layer has been made in terms of suitable parameters that qualitatively describe the occurrence of detachment. Accordingly with this method, the considerations of this paper are limited to the wall/displacement thickness zones but provide useful and well-checked results for the viscous wake and vortex shedding. It must be noted that, although some generality is lost by this, much is gained in return, since the computational (and design) criteria then may be applied both in steady and unsteady flow, and, also, both in laminar and turbulent flow. The same considerations are applicable in the wake (and its evolution), so that the airfoil drag and pressure coefficients are easily obtained. The wake geometries and evolutions follow accurately from the proposed procedure. Many other different approaches and numerical techniques are applied for the analysis of unsteady potential aerodynamic flow around a lifting body [Katz and Weihs (1978); Moran, Cole and Wahl (1980); Ardonneau (1986); Yon, Katz and Plotkin (1992); Bassanini, Casciola, Lancia and Piva (1992); Morino (1993); Hsin, Kerwin and Newman (1993); Das and Ahmed (1995)] in which the potential-based direct approach relates the unknown potential on the body sur-

face to the known boundary conditions. Usually, in this case, numerical solutions are obtained by using constant elements of discretization, and the discontinuity in potential at the trailing edge is approximated by the difference between the potentials evaluated at the centroidal control points of the contiguous elements at the trailing edge [Morino and Kuo (1974); Maskew (1982)]. Once this step is completed, these methods lead to the violation of the pressure continuity condition at the airfoil trailing edge. In order to overcome these problems, an explicit Kutta condition which should be applied, at least for unsteady large-amplitude motion of low reduced frequency, where the angle of attack is such that flow separation does not occur, has been applied successfully [Davì, Marretta and Milazzo (1997)]. A method based on a Newton-Raphson scheme has been used by Kinnas and Hsin [Kinnas and Hsin (1992)] to iterate an explicit equal pressure condition at the trailing edge. The implementation of this technique shows a slow convergence, and, more recently, a development based on the linearization of the pressure coefficient was employed by Bose [Bose (1994)]. When a more computational efficiency is required in computing the viscous flow-fields around airfoils, fundamental criteria are stated both in terms of wall shear stress (and/or intermittency) and the zones of viscous-inviscid flow interaction [Tuncer, Ekaterinaris and Platzer (1995); Okumura and Kawahara (2000); Simonetti and Ardito Marretta (2000); Levin and Shyy (2001)]. When a Reynolds-averaged Navier-Stokes solver is coupled with a potential flow panel code, an attempt to split the flow-field into viscous and inviscid flow zones leads to the objective to reduce the computational domain in which N-S equations are solved. This technique being typically connected with unsteady and low-speed airfoil flows.

2 Physical arguments and proposed criterion

When the N-S/potential flow interactive scheme (and solution) is adopted, the computational domain is partitioned into two zones, a near field and a far field zone. It is obviously recognized that a full comprehensive model of the physics of the flow field is quite far to reach, without considering and taking into account the viscous effects. In many applications, one could usefully consider the method proposed by Morino [Morino (1993)] in which the Helmholtz decomposition is capable to give both a scalar and a vector potential function. Computational time reduction may be produced through a differ-

ent recursive scheme when applied for airfoils, consisting of:

1. Potential flow-field solved to find the surface velocity distribution.
2. Boundary layer equations solution in terms of the above mentioned velocities.
3. Updating the boundary conditions for a recursive computational scheme.

Once the parameters linked to the boundary layer are defined (displacement, momentum and energy dissipation thicknesses in Eqs. 1(a-c), respectively), these quantities will be useful to compute the friction drag and energy losses (here mass and heat transfers are absent) [Young (1989)]. Assuming the flow as incompressible and two-dimensional:

$$\partial_1 = \int_0^{\infty} \left(1 - \frac{\rho u}{\rho_e U_e}\right) dz \simeq \int_0^{\delta} \left(1 - \frac{u}{U_e}\right) dz, \quad (1a)$$

$$\partial_2 = \frac{1}{U^2} \int_0^{\infty} u(U - u) dz, \quad (1b)$$

$$\partial_3 = \frac{1}{U^3} \int_0^{\infty} u(U^2 - u^2) dz. \quad (1c)$$

A reasonable point of departure is to consider the new airfoil section (and the wake geometry), once the displacement thickness distribution is now obtained. Although this procedure is widely applied and gives consistent results, it is strongly affected, from computational point of view, by cost and time constraints. Indeed, it will be necessary re-computing the new versors to the airfoil surface at each recursive computational step, giving as effect, a substantial alteration of the actual flow variables.

Alternatively, as it will be shown in this paper, a different approach, under the above mentioned hypotheses, is suitable to provide useful results very close to those theoretically and experimentally obtained. Following Lighthill's method, we leave unchanged the airfoil surface and collect the effects of displacement thickness through a "normal velocity field" to the airfoil surface. Outside the boundary layer, the velocity normal component is:

$$\begin{aligned} w &= \int_0^z \frac{\partial w}{\partial z} dz = - \int_0^z \frac{\partial u}{\partial x} dz, \\ &= - \frac{dU_e}{dx} z + \frac{\partial}{\partial x} \int_0^z (U_e - u) dz, \\ &= - \frac{dU_e}{dx} z + \frac{\partial}{\partial x} \int_0^{\infty} (U_e - u) dz, \end{aligned} \quad (2)$$

since z is large enough for $U - u$ to vanish, and hence for z to be replaced by ∞ in the last integral in accordance with the conventions of boundary layer theory. As Lighthill wrote, ... *this additional outflow* (linked to the presence of the boundary layer, n.o.w.) *is exactly "as if" the irrotational flow around the body were supplemented by the effect of a surface distribution of sources...* The strength, σ , per unit area, of that distribution is:

$$\sigma = \frac{d}{dx} \int_0^{\infty} (U_e - u) dz = \frac{d}{dx} (U_e \delta_1). \quad (3)$$

The actual boundary conditions will be rearranged as:

$$\frac{\partial(\Phi + \Phi_{\infty})}{\partial n} = V_n \quad (4)$$

being V_n equal to $\partial(U_e \delta_1)/\partial s$. Note that the Lighthill's transpiration velocity does not violate the Helmholtz decomposition.

2.1 Boundary-layer model

Here, the recursive computational procedure for the viscous enhancement of the potential flow-field follows the scheme:

Many factors may considerably affect the transition process: the surface pressure gradient, the airfoil surface roughness and bending, heat transfer, flow compressibility. Taking into account Rayleigh flexus point criterion [Rayleigh (1913)] and the statements of Sommerfeld [Sommerfeld (1908)], the Prandtl's equation [Prandtl (1933)], written at the surface, becomes (with obvious meaning of symbols):

$$\mu \left(\frac{\partial^2 u}{\partial z^2} \right) = \frac{\partial p}{\partial x}. \quad (5)$$

In the restricted range of Reynolds numbers between 10^6 and 10^7 , it is reasonable to admit the transition limit be

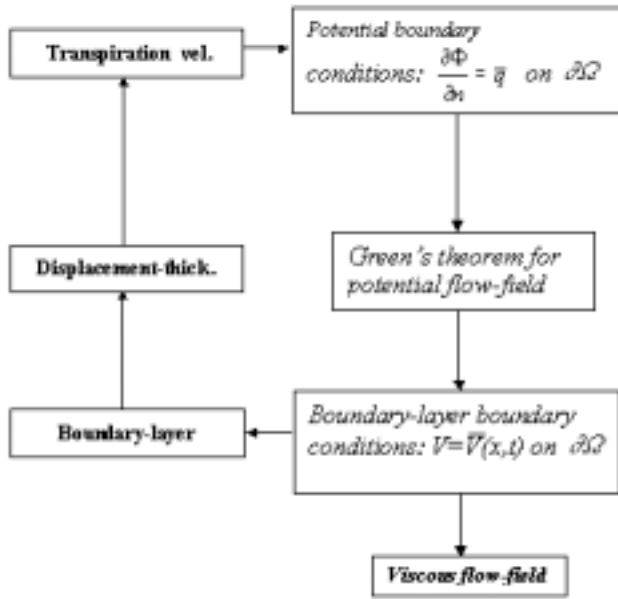


Figure 1 : Recursive computational scheme

coincident with the minimum pressure point [Schlichting (1968)]. Starting with these considerations, laminar and turbulent distributions, fore and aft this point, are supposed respectively, for the boundary layer distribution. Thwaites suggests [Thwaites (1949), (1952)], for the laminar distribution, to take into account for the two parameters, l and m given below, the following relationships:

$$l = \frac{\delta_2}{U} \left(\frac{\partial u}{\partial z} \right)_w = \frac{\delta_2 \tau_w}{U \mu}, \tag{6a}$$

$$m = \frac{\delta_2^2}{U} \left(\frac{\partial^2 u}{\partial z^2} \right)_w. \tag{6b}$$

Where τ_w indicates the wall shear stress. The two parameters l and m are strictly connected with the friction stress and the pressure gradient, respectively. One easily obtains (from $v \partial^2 u / \partial z^2 = -U \partial U / \partial x$):

$$m = -\frac{\delta_2^2}{v} \left(\frac{\partial U}{\partial x} \right). \tag{6c}$$

By doing so, the only hypothesis carried out is that the velocity contours of the boundary layer distribution admit the same parameter, being m the chosen one (single-parameter family description). The momentum integral equation becomes:

$$U \frac{\partial \delta_2}{\partial x} + \frac{\delta_2}{U} \frac{dU}{dx} (H_{12} + 2) = \frac{\tau_w}{U^2 \rho} \tag{7}$$

where H_{12} represents the displacement/momentum thicknesses ratio; the Eq. 6, in terms of l and m , is now attained:

$$U \frac{d\delta_2^2}{dx} + 2\nu [m(H_{12} + 2) + l] = \nu L(m) \tag{8}$$

It is found for a wide range of solutions, both theoretical and nearly exact ones, the values $L(m)$ are those possessed by the following simple relationship:

$$L(m) = 0.45 + 6m. \tag{9}$$

Through the Eqs. 8 and 9, we easily find:

$$U \frac{d}{dx} (U^6 \delta_2^2) = 0.45 \nu U^5 \nu L(m). \tag{10}$$

By integrating the Eq. 10 from the stagnation point ($x = 0$) up to the generic coordinate, x_1 , the equation for $\delta_2^2(x_1)$ is finally obtained:

$$\delta_2^2(x_1) = 0.45 \frac{\nu}{U^6} \int_0^{x_1} U^5 dx. \tag{11}$$

Once the value of $\delta_2^2(x_1)$ is computed, the parameter value of m is attained and the recursive scheme, shown in Fig. 1, provides L , H_{12} , τ_w and δ_1 , consequently (see Appendix).

The method proposed by Truckenbrodt [Truckenbrodt (1952)] for the turbulent boundary layer has been adopted in this paper and considered with the presence of adverse gradient pressure. Differently from other nearly exact methods, such as those of Buri [Buri (1931)], von Doenhoff and Tetervin [von Doenhoff and Tetervin (1943)] and Garner [Garner (1944)], in the adopted method, the starting point is not the momentum integral equation but the energy integral equation, i.e.:

$$\frac{1}{2} \rho \frac{d}{dx} \int_0^\infty u(U^2 - u^2) dz = \mu \int_0^\infty \left(\frac{\partial u}{\partial z} \right)^2 dz. \tag{12}$$

which can be expressed in terms of the correspondent thickness, δ_3 , as:

$$\frac{1}{U^3} \frac{d}{dx} (U^3 \delta_3) = 2 \frac{d_1 + t_1}{\rho U^3}. \quad (13)$$

The quantity on the right-hand term is equivalent to the dimensionless friction energy due to the boundary layer shear stress. More in detail, d_1 and t_1 ($t_1 \ll d_1$) denote heat losses and turbulent energy, respectively. Following Rotta [Rotta (1956)], the Reynolds number, $U\delta_2/\nu$ may be introduced:

$$\frac{d_1}{\rho U^3} = \frac{0.56 \cdot 10^{-2}}{(U\delta_2/\nu)}, \quad (14a)$$

$$\frac{\tau_0}{\rho U^2} = 0.123 \cdot 10^{-0.678 H_{12}} \left(\frac{U\delta_2}{\nu} \right)^{-0.268}. \quad (14b)$$

Finally, combining the Eqs. 13 and 14, the integration in closed form yields:

$$\frac{\delta_2(x)}{l} = \left(\frac{U}{U_\infty} \right)^{-3} \left[C_1^* + \left(\frac{c_f}{2} \right)^{7/6} \int_{x_t/l}^{x/l} \left(\frac{U}{U_\infty} \right)^{10/3} d \left(\frac{x}{l} \right) \right]^{6/7}. \quad (15)$$

In the Eq. 15, once the transition point is located on the coordinate $x = x_t$, c_f is the turbulent friction coefficient, while the constant, C_1^* , takes into account the laminar zone of the boundary layer (see Appendix). A simple gaussian quadrature is suitable to resolve the Eq. 15 and we easily find the momentum thickness and the displacement one as well:

$$\frac{d\delta_2}{dx} + (H_{12} + 2) \frac{\delta_2}{U} \frac{dU}{dx} = \frac{\tau_0}{\rho U^2}. \quad (16)$$

Subtracting this from Eq. 13, with simple rearrangements, one obtains:

$$\delta_2 \frac{dH_{32}}{dx} = (H_{12} - 1) H_{32} \frac{\delta_2}{U} \frac{dU}{dx} + 2 \frac{d_1 + t_1}{\rho U^3} - H_{32} \frac{\tau_0}{\rho U^2}. \quad (17)$$

where H_{32} denotes the ratio δ_3/δ_2 ; a further expression of the Eq. 17 may be found whereas the Reynolds number, $U\delta_2/\nu$, and the shape function, H_{12} are introduced:

$$\left(\frac{U\delta_2}{\nu} \right)^{1/6} \delta_2 \frac{dL}{dx} = \left(\frac{U\delta_2}{\nu} \right)^{1/6} \frac{\delta_2}{U} \frac{dU}{dx} - K(L). \quad (18)$$

where the expression of L is given in Appendix.

In order to accomplish the vanishing pressure gradient (limit case of flat plate), the suggested value for $(H_{32})_0$ has to be taken ≈ 1.73 . Now, it will suffice to take back the (well-approximated) linear function of $K(L)$ (for its coefficients, see Appendix) from specific milestone literature to find easily:

$$\xi = \left[C_1^* + \left(\frac{c_f}{2} \right)^{7/6} \int_{x_t/l}^{x/l} \left(\frac{U}{U_\infty} \right)^{10/3} d \left(\frac{x}{l} \right) \right]^4. \quad (19)$$

where ξ is a convenient current coordinate. The following last equation relates L to the velocity distribution along the current coordinate:

$$L = \frac{\xi_1}{\xi} L_1 + \ln \frac{U(\xi)}{U_1} + \frac{1}{\xi} \int_{\xi_1}^{\xi} \left[b(\xi) - \ln \frac{U(\xi)}{U_1(\xi_1)} \right] d\xi. \quad (20)$$

In the Eq. 20, the subscript 1 is connected to scalar quantities computed at the transition point x_t . Once L is known, the previous equations give the values of H_{12} (moreover, because of in the present discussion, both of them are shape functions). In order to accomplish the first objective of this paper, once H_{12} and δ_2 are known, the displacement thickness is found to give the response for the detachment of the vein for a range of H_{12} between 1.8 and 2.4.

3 Results validation and discussions

The described criterion has been applied, in the present paper, to analyze the flow-field around a wing section NACA 0012. The choice is fallen on this wing family for many reasons. First, their large employment in specific aeronautical industries, their wide application in literature (both theoretically and experimentally) and, last but not least, because of this family of wing sections is very far from massive separation when attacked by flows

under confined range of angles of incidence. Here, we want to address the numerical results of the present formulation for the viscous unsteady motion. As previously underlined, the distinguishing difference between the present criterion and those found in literature is related to the choice of the model to develop and enhance the potential velocity formulation. Differently from Cebeci et al. [Cebeci, Platzer, Jang and Chen (1993)] and Tuncer and Ekaterinaris [Tuncer and Ekaterinaris (1995)] (their methods remain valid but, unfortunately, the local and inner solution is needed to predict the transition point even though without constraints about the nature of the boundary layer itself), the procedure suggested in this work is to adopt, for the boundary layer solution, an approximated solution based on the integral equations of momentum (*MIE*) and kinetic energy (*KIE*). We want to point out that, although this criterion loses information about the inner and local behavior of the boundary layer, nevertheless, at the same time, it is suitable to diminish greatly the computational effort and, however, compute accurately the airfoil performance parameters. Much is gained in return; to demonstrate this, 34 elements of discretization for the airfoil are enough to a fast and well-checked convergence (the recursive process settled out by the authors is capable to collect, as input, shape functions of higher order). As regards the wake (both inviscid and viscous), the panelization used deals with a linear distribution of vortices while the viscous implementation has been carried out for a plausible range of Reynolds number [$3 \times 10^6 \div 9 \times 10^6$] in agreement with the chosen model of the friction coefficient. For the sake of simplicity (and to give accurate comparison of the results), the range of the angle of attack was confined up to 11° . To calculate the airfoil responses, the recursive computational process runs until the non-dimensional time, $t * U/\text{chord}$, reaches 200 units along a non-dimensional time interval $\Delta\tau = 1$. This seems fast enough for the flow leaving the airfoil to reach a distance equal to a 4 chords length from the trailing edge. The method proposed seems robust and its high portability are proved through very few potential-viscous iterations needed to reach the transpiration velocity convergence (See Figs. 2-4). Note that Figs. 2-4 show the velocity transpiration versus the viscous iterations considered at three different (and particular) zones of the airfoil, such as the trailing and leading edges and the maximum thick. Fig. 5 displays the NACA 0012 airfoil polar for $Re=3*10^6$; the comparison shows a good agreement with experimental

results.

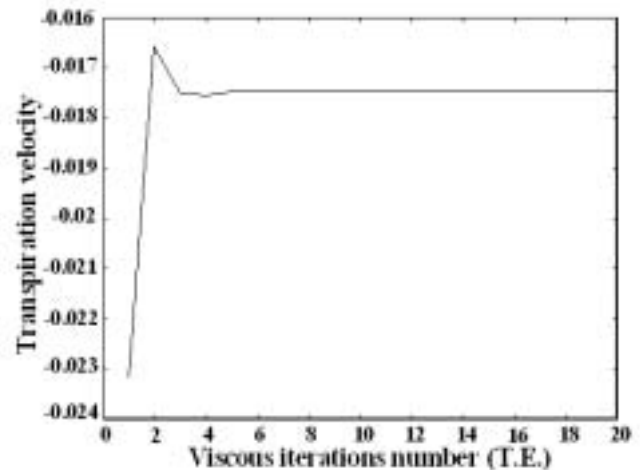


Figure 2 : Recursive convergence at the trailing edge

It must be noted a small discrepancy of the present method to fit the experimental results around the vanishing value of the lift coefficient. This is to be tied to the chosen Reynolds number; when Re is approaching the value mentioned above,

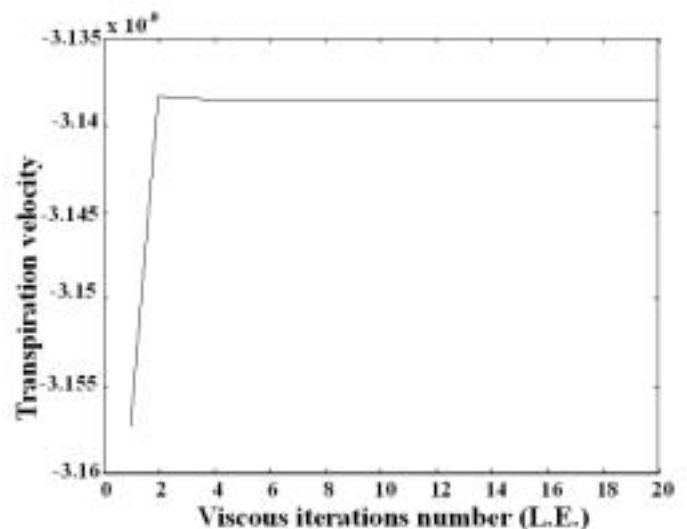


Figure 3 : Recursive convergence at the leading edge

the method of Truckembrodt [Truckenbrodt (1952)], for the friction coefficient, is very close to its limit of availability. The same features are shown in Fig. 6 for a Reynolds number of $9*10^6$.

We may view the calculations sequence is stopped when the lift coefficient is equal to 1.2. Note, on the other hand,

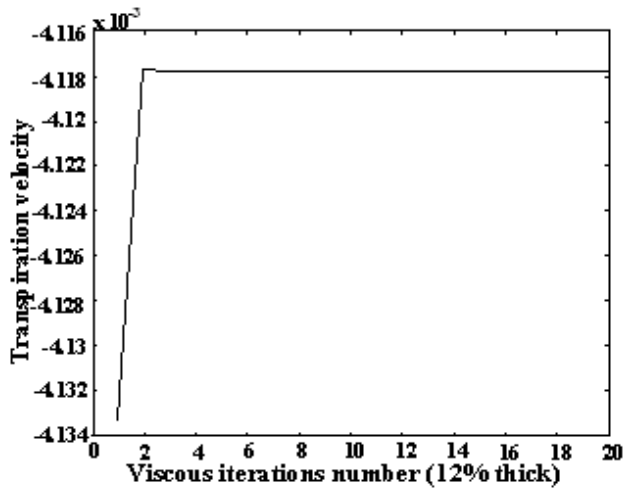


Figure 4 : Recursive convergence at 12% thick

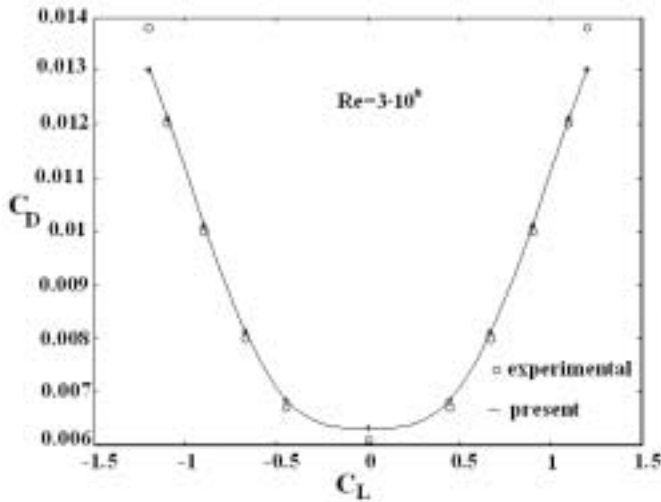


Figure 5 : Airfoil polar ($Re=3 \cdot 10^6$)

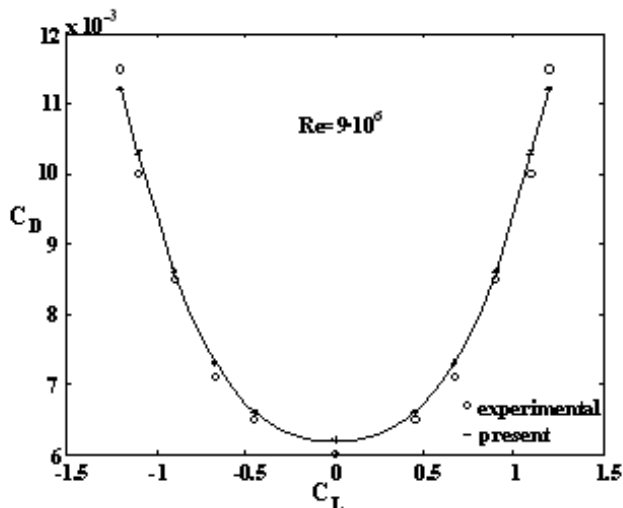


Figure 6 : Airfoil polar ($Re=9 \cdot 10^6$)

that this implies two important factors: first, an angle of attack equal to 11° , for which the detachment may be in progress near the trailing edge and, secondly, the shape drag contribution is growing up more quickly than the friction drag coefficient. As regards the viscous effects on the lift (attached flow), the pressure coefficient (angle of attack, $\alpha = 7^\circ$) is shown in Fig. 7: results obtained with this procedure give a viscous lift coefficient of 0.798 against a potential one of 0.8.

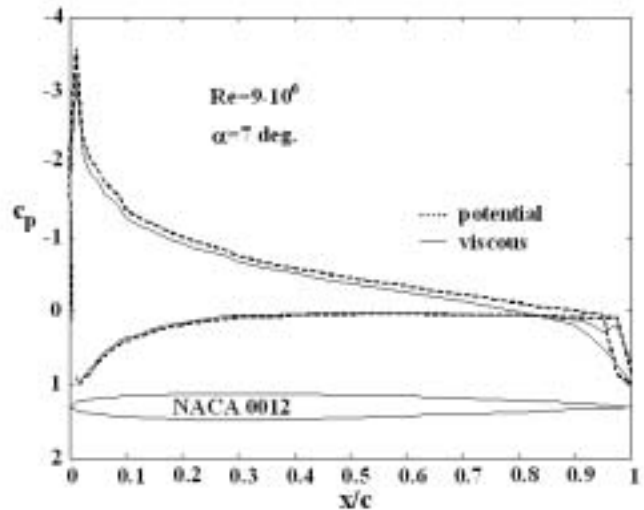


Figure 7 : Airfoil pressure distribution

Here, the slight deviation is linked to the presence of boundary layer; in fact, for the airfoil considered and with $\alpha = 7^\circ$, this guarantees a smaller reduction of the pressure differences between the upper and lower regions of the airfoil than those computed by a full-potential code. The accuracy of the computed aerodynamic performance of the airfoil does not deteriorate when the vortical wake field is described, but similarly, the present criterion computations were found to be insensitive for its (very good) quality of response to the range of unsteady parameters of motion. It is clearly seen that the proposed method is highly accurate and stable when the comparison of the present results is made with those of Katz and Weihs [Katz and Weihs (1978)] and Tuncer and Ekaterinaris [Tuncer and Ekaterinaris (1995)]. Different wake geometries, computed for this airfoil, are presented in the following figures/images. Experimental data support this criterion in the range of values including the same free-stream velocity, reduced frequency, ω , and time computational step, $\Delta\tau = U_\infty \Delta t / \text{chord}$. Here, the analysis is intended to describe the unsteady and viscous correlation

between the range of the angle of attack (linear range of the slope $C_L-\alpha$ curve) with the evolution (in time and space) of the wake past the airfoil. Although the model of Tuncer and Ekaterinaris takes also into account the compressibility effect, a comparison with the present results is done when the Mach number is put equal to 0.3. More in detail, Fig. 8 presents, for $t = 200$, $\Delta\tau = 1$, $\omega = .2$, $h/c = .16$ and $Re=9*10^6$, the wake geometries for potential and viscous solutions which are, not surprisingly, about merging because of the relatively slow reduced frequency used.

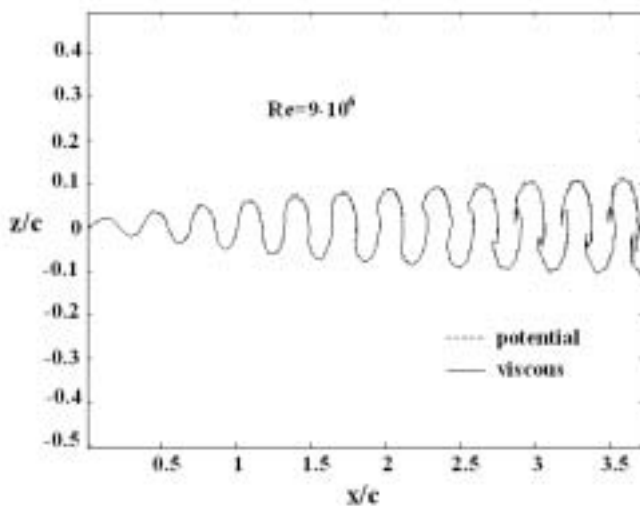


Figure 8 : Wake geometries comparison

A closer-view analysis may highlight the differences between the two vortical shape as shown in Fig. 9. The present method thus leads to the same behavior (and the same conclusions) shown in Figs. 10(a-b), 11(a-b) and 12(a-b), for the experimental and computed wake geometries, when the same airfoil and the same unsteady parameters of Katz and Weihs [Katz and Weihs (1978)] are employed, respectively ($t = 200$, $\Delta\tau = .009$, $U_\infty/\text{chord}=1.56\text{sec}^{-1}$, $\omega = 8.5789$, $h/c = .019$, $Re=9*10^6$; $t = 200$, $\Delta\tau = .00225$, $U_\infty/\text{chord}=6.24\text{sec}^{-1}$, $\omega = 2.15$, $h/c = .019$, $Re=9*10^6$ and $t = 200$, $\Delta\tau = .00065$, $U_\infty/\text{chord}=21.3\text{sec}^{-1}$, $\omega = 0.65$, $h/c = .019$; $Re=9*10^6$).

However, for mostly attached flows up to $\alpha=11^\circ$, the accuracy of the computed wake evolutions and shapes does not degrade more than very slight percentage. At higher incidences, the criterion proposed ceases to be efficient but this limit was never reached and considered at the beginnings of this paper.

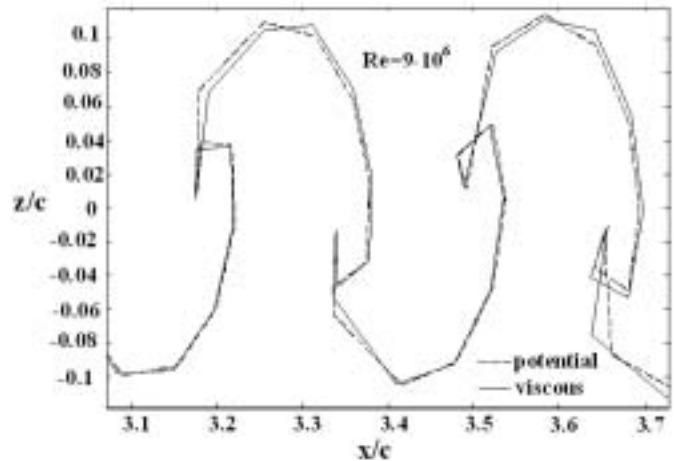


Figure 9 : Closer view of Fig. 8

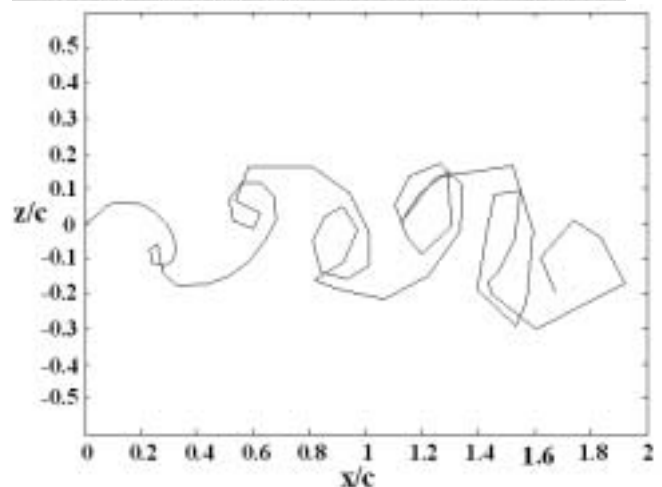


Figure 10 : (a) Leaving wake evolution (experimentally); (b) Leaving wake evolution (computationally).

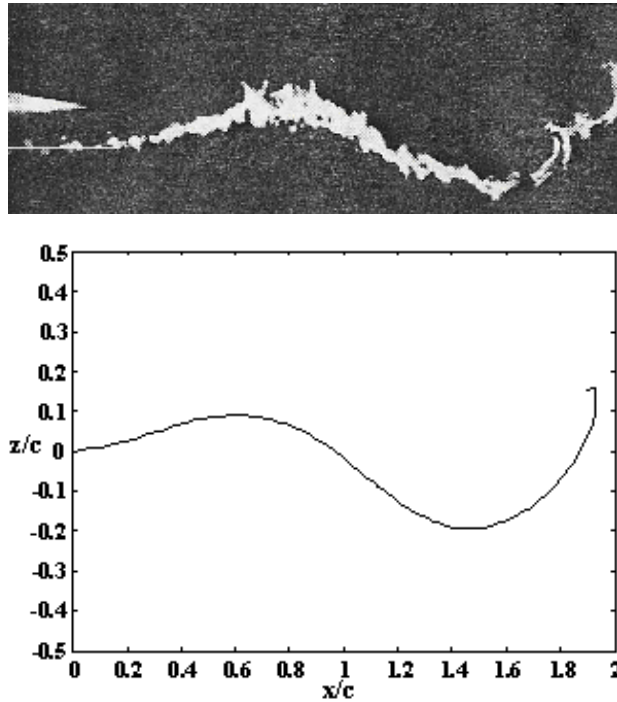


Figure 11 : (a) Leaving wake evolution (experimentally);
(b) Leaving wake evolution (computationally).

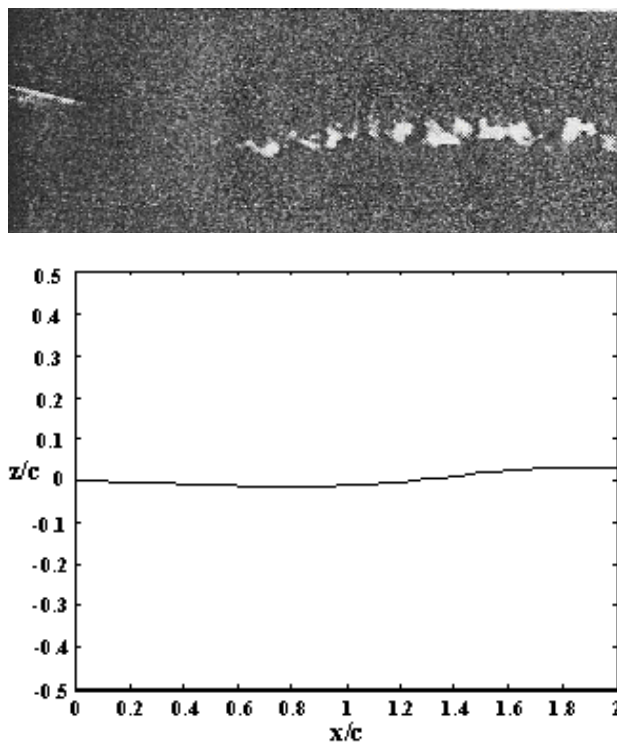


Figure 12 : (a) Leaving wake evolution (experimentally);
(b) Leaving wake evolution (computationally).

4 Conclusions

In this paper, we have developed a useful criterion for the design of airfoils in unsteady and viscous flows. This criterion confines its methodologies to the close proximity of the laminar and turbulent boundary layer and it shows good efficiency in predicting and calculating the wake evolution regions in a wide range of operating unsteady parameters. Also, the criterion is capable of predicting low Mach number, attached flow-fields as accurately as the full N-S solutions when the massive flow separation is avoided. The agreement of the present results with those empirically and theoretically determined is very accurate for attached flows and well within the general range of the boundary layer correlations and the angles of attack of the airfoils. Although this criterion does not highlight the behavior of the inner zones of the displacement thickness, a plausibility argument was given as to why this behavior is reasonable even though few solid theoretical basis can be offered. The satisfying features of this criterion are that few determined (critical) values are required for the calculation of the aerodynamic performance parameters of the airfoils and it is about 50% more efficient in computational output speed than the Navier-Stokes/potential flow interactive solutions.

Appendix

In this Appendix we show the explicit expressions for the above mentioned parameters throughout the text.

Table 1 : Values of L , m and H_{12}

m	l	H_{12}
-0.25	0.500	2.00
-0.20	0.463	2.07
-0.14	0.404	2.18
-0.12	0.382	2.23
-0.10	0.359	2.28
-0.080	0.333	2.34
-0.064	0.313	2.39
-0.048	0.291	2.44
-0.032	0.268	2.49
-0.016	0.244	2.55
0	0.220	2.61
0.016	0.195	2.67
0.032	0.168	2.75
0.040	0.153	2.81
0.048	0.138	2.87
0.056	0.122	2.94
0.060	0.113	2.99
0.064	0.104	3.04
0.068	0.095	3.09
0.072	0.085	3.15
0.076	0.072	3.22
0.080	0.056	3.30
0.084	0.038	3.39
0.086	0.027	3.44
0.088	0.015	3.49
0.090	0	3.55

$$C_1^* = \left[\frac{1}{2} c_{fl} \left(\int_0^{x_i/l} \left(\frac{U}{U_\infty} \right)^5 d \left(\frac{x}{l} \right) \right)^{1/2} \right]^{7/6}, \quad (a)$$

$$L = \int_{(H_{32})_0}^{H_{32}} \frac{dH_{32}}{(H_{12} - 1)H_{32}}, \quad (b)$$

$$K(L) = a(L - b), \quad (c)$$

$$a = 0.0304; \quad b = 0.07 \log(U\delta_2/\nu) - 0.23.$$

References:

Ardonceau, P. L. (1986): Computation of the potential flow over airfoils with cusped or thin trailing edges.

AIAA Journal, vol. 24, pp. 1375-1377.

Bassanini, P.; Casciola, C. M.; Lancia, M. R.; Piva, R. (1992): A boundary integral formulation for the kinetic field in aerodynamics. II. Applications to unsteady 2D flows. *Eur. J. Mech. B/Fluids*, vol. 11, pp. 69-92.

Buri, A. (1931): Eine berechnungsgrundlage für die turbulente grenzschicht bei beschleunigter und verzögerter Strömung. *J ZFW*, vol. 9, pp. 97-99.

Cebeci, T.; Platzer, M. F.; Jang, H. M.; Chen, H. H. (1993): An inviscid-viscous interaction approach to the calculation on dynamic stall initiation on airfoils. *J of Turbomachinery*, vol. 115, pp. 714-723.

Das, A.; Ahmed, S. R. (1995): Progress on the boundary element method to study the disturbance fields of bodies moving in an unbounded medium. *Computational Mechanics*, vol. 15, pp. 315-333.

Davi, G.; Marretta, R.; Milazzo, A. (1997): Explicit Kutta condition for unsteady two-dimensional high-order potential BEM. *AIAA Journal*, vol. 35, pp. 1080-1081.

von Doenhoff, A. E.; Tetervin, N. (1943): Determination of general relations for the behavior of turbulent boundary layers. In: NACA (ed) *NACA Report*, vol. 772.

Garner, H. C. (1944): The development of turbulent boundary layers. *J ARC RM*, vol. 2133.

Hsin, C. Y.; Kerwin, J. E.; Newman, J.N. (1993): A higher-order panel method based on B-splines. In: *Proceedings of the 6th Int. Conf. on Numerical Ship Hydrodynamics*, The University of Iowa, Iowa City, pp. 133-151.

Katz, J.; Weihs, D. (1978): Behavior of vortex wakes from oscillating airfoils. *AIAA Journal*, vol. 15, pp. 861-863.

Kinnas, A. S.; Hsin, C. Y. (1992): Boundary Element Method for the analysis of unsteady flow around extreme propeller geometries. *AIAA Journal*, Vol. 30, pp. 688-696.

Lighthill, M. J. (1958): On displacement thickness. *J of Fluid Mechanics*, vol. 4, pp. 383-392.

Levin, O.; Shyy, W. (2001): Optimization of a low Reynolds number airfoil with flexible membrane. *CMES: Computer Modeling in Engineering & Sciences*, vol. 2, No. 4, pp. 523-536.

Maskew, B. (1987): Program VSAERO theory document. In: Nasa (ed) Nasa CR 4023.

- Moran, J.; Cole, K.; Wahl, D.** (1980): Analysis of two-dimensional incompressible flows by a subsurface panel method. *AIAA Journal*, vol. 18, pp. 526-533.
- Morino, L.** (1993): Boundary integral equations in aerodynamics. *J of Applied Mechanics*, vol. 46, pp. 445-466.
- Morino, L.; Kuo, C. C.** (1974): Subsonic potential aerodynamics for complex configurations: a general theory. *AIAA Journal*, vol. 12, pp. 191-194.
- Okumura, H.; Kawahara, M.** (2000): Shape optimization of body located in incompressible Navier-Stokes flow based on optimal control theory. *CMES: Computer Modeling in Engineering & Sciences*, vol. 1, No. 2, pp. 71-78.
- Prandtl, L.** (1933): Neuere ergebnisse der turbulenzforschung. *Z VDI*, vol. 77, pp. 105-114.
- Rayleigh, J. W. S.** (1913): On the stability of certain fluid motions. *Proc. Math. Soc.*, London, vol. 6, pp. 474-487.
- Rotta, J.** (1956): Experimenteller beitrag zur entstehung turbulenter strömung im rohr. *J Ing. Arch.*, vol. 24, pp. 258-281.
- Sajben, M.; Liao, Y.** (1995): Criterion for the detachment of laminar and turbulent boundary layers. *AIAA Journal*, vol. 33, pp. 2114-2119.
- Schlichting, H.; Kestin, J.** (1968): Boundary layer theory. In: McGraw-Hill (ed) *Boundary layer theory*, McGraw-Hill Company, London, 6th ed., pp. 467-479 and also pp. 626-644.
- Simonetti, F.; Ardito Marretta, R.** (2000): A numerical variational approach for rotor-propeller aerodynamics in axial flight. *CMES: Computer Modeling in Engineering & Sciences*, vol. 1, No. 3, pp. 81-90.
- Sommerfeld, A.** (1908): Ein beitrag zur hydrodynamischen erklärang der turbulenten flüssigkeitsbewegungen. In: CIM (ed) *Atti del 4 Congr. Internat. dei Mat.*, Roma, vol. 3, pp. 116-124.
- Thwaites, B.** (1949): Approximate calculation of the laminar boundary layer. *Aeronautical Journal Quarterly*, vol. 1, pp. 245-280.
- Thwaites, B.** (1952): On the momentum equation in laminar boundary layer flow. A new method of uniparametric calculation. *ARC RM*, vol. 2514.
- Truckenbrodt, E.** (1952): Ein quadraturverfahren zur berechnung der laminaren und turbulenten reibungsschicht bei ebener und rotationssymmetrischer strömung. *J Ing. Arch.*, vol. 20, pp. 211-228.
- Tuncer, I. H.; Ekaterinaris, J. A.; Platzer, F.** (1995): Viscous-inviscid interaction method for unsteady low-speed airfoil flows. *AIAA Journal*, vol. 33, pp. 151-154.
- Yon, S.; Katz, J.; Plotkin, A.** (1992): Effect of airfoils (trailing-edge) thickness on the numerical solution of panel methods based on the Dirichlet boundary condition. *AIAA Journal*, vol. 30, pp. 697-702.
- Young, A. D.** (1989): Boundary layer. In: AIAA (ed) *AIAA Educational Series*, Ed. 1989, pp. 272-293.

